Research Article

Journal of Environmental Nanotechnology

Tetraethylenepentamine-modified Halloysite Clay Nanotubes for CO_2 Capture

Nalinkanth Veerabadran Ghone*, S. Jagannath and Kishore

Department of Chemical Engineering, Sri Sivasubramaniya Nadar College of Engineering, Kalavakkam, TN, India

Received: 26.01.2026 Accepted: 30.02.2026 Published: 30.03.2026

*nalinkanthv@ssn.edu.in

ABSTRACT

Halloysite clay nanotubes, which occur naturally in a nanotubular form, possess high inherent adsorption capability due to their tubular morphology, high porosity, and large specific surface area. To enhance the application of these nanotubes in CO_2 capture, a novel approach of immobilizing tetraethylenepentamine (TEPA) onto alkali-modified halloysite nanotubes via the impregnation method was employed. Alkali modification of halloysite nanotubes using KOH was carried out to activate the multilayered surface for impregnation. The prepared halloysite clay solid sorbents were characterized using FTIR, SEM, and EDAX, and were further tested for their potential in CO_2 capture. The adsorption capacity of halloysite significantly increased from 6.36 mmol CO_2/g of adsorbent to 10.23 mmol CO_2/g of adsorbent upon modification with TEPA. In conclusion, TEPA-impregnated halloysite represents a promising nanomaterial for CO_2 capture, and further techno-economic studies may yield a viable and flexible capture system suitable for a wide range of process industries.

Keywords: Halloysite clay; Nanotube; Solid sorbent; CO_2 capture; Tetraethylenepentamine.

1. INTRODUCTION

Carbon dioxide (CO_2), a major greenhouse gas, is one of the chief causes of global warming (Jacobson, 2009). The presence of CO_2 in the atmosphere has been increasing at a higher rate since the advent of the Industrial Revolution. Furthermore, urbanization and the reduction of green cover on Earth due to deforestation have worsened the situation. As per reports from the National Oceanic and Atmospheric Administration, US Department of Commerce, the atmospheric CO_2 has already crossed the redline level of 400 ppm in 2016, and the recent average value for 2022 is 417 ppm. At the current rate, it is expected to reach 500 ppm by 2038. This alarming increase in atmospheric CO_2 is demanding attention from researchers to develop robust and economical CO_2 capture and storage (CCS) technologies. In CCS technologies, CO_2 capture is an important integral part, which alone accounts for 75% of the entire cost (Olajire, 2007). Around 40% of total CO_2 emissions into the atmosphere are contributed by fossil fuel-based power plants alone. It is estimated that the flue gas from these power plant industries contains around 15% of CO_2 (Mondal *et al.* 2012; Leung *et al.* 2014). Hence, technologies based on post-combustion capture of CO_2 are the most favorable, rapid, and economical for reducing the current CO_2 emissions when compared to other technologies such as pre-combustion capture, oxy-fuel combustion, and direct air capture (Lee and Park, 2015; Raganati *et al.* 2021; Saenz Cavazos, 2023). Among those technologies, different choices are available based on major separation techniques such as absorption using solvents, membranes, cryogenics, adsorption by solid sorbents, and the calcium looping cycle (Dhoke *et al.* 2021). Absorption using amine solvents is the most mature technology for post-combustion capture; however, it has several drawbacks, including high energy demand for solvent regeneration, corrosion problems, solvent losses, and degradation in the presence of oxygen in the flue gas, and serious environmental concerns related to amine disposal (Gargiulo *et al.* 2018). Adsorption on solid sorbents is an attractive alternative as it provides several advantages, such as significant energy savings and ease of retrofitting to existing process plants due to more options for regeneration methods and reactor types (Webley, 2014). A vast number of studies have reported several carbonaceous (activated carbons, ordered porous carbons, carbon nanotubes, graphene) and non-carbonaceous materials (zeolites, silica materials, metal organic frameworks, alkali metals, metal oxides, and polymers) for the application of carbon capture (Lee and Park, 2015; Lou *et al.* 2020; Zhao *et al.* 2021). Amine functionalization of these solid porous adsorbents has enhanced their CO_2 adsorption capacity (Chen *et al.* 2017; Nie *et al.* 2018; Zhao *et al.* 2021). In general, the amine functionalization is done by three methods, namely the direct synthesis method, impregnation, and grafting method. Impregnation is a facile method for amine functionalization, in which non-covalent interactions of the amine group happen with adsorbents (Ye *et al.* 2012). It has been shown that alkali activation prior to impregnation with amine agent further improves the CO_2 adsorption capacity for carbon nanotubes due to the formation of a more porous structure during activation (Irani *et al.* 2017). In the current work, alkali

activation followed by amine impregnation is used to enhance the absorption capacity of halloysite clay nanotube.

Halloysite nanotube (HNT) is a naturally available clay material formed by the rolling of alumina silicate sheets due to weathering. The wall of these tubes has more than 15 layers, with siloxane groups on the outside of the tube and hydroxyl groups attached to alumina in the inside of the tube. Its lumen diameter is 15–30 nm, outer diameter 50–100 nm, and length varies from 100 nm to a couple of microns. Owing to its natural availability, low cost, high adsorption capabilities, and ease of modification, these are considered as promising nanomaterials for multifarious applications (Tharmavaram *et al*. 2018), such as controlled drug delivery (Veerabadran *et al*. 2007; Veerabadran *et al.* 2009; Abdullayev *et al.* 2016), life science applications (Santos *et al.* 2018), and making smart nanocomposites (Wu *et al.* 2019; Bertolino *et al*. 2020). One of the earliest studies on the utilization of HNTs for CO_2 adsorption was reported a decade ago, in which activation of halloysite by calcination before (3-aminopropyl) triethoxysilane (APTES) surface modification has enhanced the adsorption of CO_2 (Zhang *et al*. 2014). Without any activation, surface-modified HNTs with APTES showed preferential adsorption of isotopes of CO_2 (12C16O2,13C16O2 and 12C16O18O) (Jana *et al.* 2015). In another study, APTES grafted HNT was compared with polyethyleneimine (PEI)-impregnated HNT for the adsorption of CO_2 (Kim *et al.* 2016). It was found that the adsorption of PEI-HNT and APTES grafted HNT is 0.21 mmoleCO_2/g of adsorbent and 0.15 mmole CO_2/g of adsorbent, respectively. In another study, the adsorption of CO_2 by PEI-modified HNT is found to be 1.25 mmole CO_2/g (Cai *et al.* 2015). At high pressure of CO_2 (30 bar), the adsorption capacity of HNT at 0 °C is found to be 6.17 mmole CO_2/g of adsorbent, and at 25 °C it is reduced to 3.4 mmole CO_2/g of adsorbent (Ramadass *et al.* 2018). In another interesting recent study, the lumen of HNT was used for loading HKUST-1, a metal-organic framework, and the surface was modified with APTES. It was shown that CO_2 adsorption increased with loading of HKUST-1, and further enhancement was observed with surface modification by APTES (Park *et al*. 2022). As per the above review of literature on CO_2 adsorption by HNT, only PEI and APTES amine have been explored. To further enhance the CO_2 adsorption by HNT, it is necessary to understand the nanoscience of amine impregnation and the right selection of amine according to the pore size of the adsorbent. Bigger amine species like PEI can easily block the mesopores of HNT, which may result in a decrease in the exposed organic amine capture sites (Chen and Bhattacharjee, 2017). Hence, prior activation of HNT before amine impregnation and the right size selection of amine may reduce pore blockage and expose more organic amine capture sites for CO_2 capture. Among the commonly used amine species, TEPA-modified adsorbents exhibit a higher CO_2 adsorption capacity due to their linear nature and less conglomeration of amine species when it is supported on adsorbent (Irani *et al*. 2017; Ye *et al.* 2012; Liu *et al.* 2014; Liu *et al.* 2014a). In this work, a potassium hydroxide-based alkali activation method has been used to activate HNT (KOH-HNT), followed by TEPA impregnation for preparing the adsorbents (TEPA-HNTs), and tested for CO_2 capture. To the best of current knowledge, KOH activation followed by TEPA impregnation of HNTs for CO_2 capture has not been reported previously.

2. MATERIALS AND METHODS

2.1 Materials

Halloysite nanotubes were supplied by Applied Minerals Inc., NY, USA, and used without further processing. TEPA, KOH, and other chemicals of analytical grade were purchased from Sigma-Aldrich. CO_2 and N_2 used for the studies were obtained from Bharath Oxygen Company, Chennai, India.

2.2 Alkali Activation of HNT

Alkali activation of the HNTs was performed by mixing KOH and HNTs at an activating agent/HNT ratio of 6:1 in 50 ml of ethanol. Then the chemicals were stirred for 6 h at room temperature and dried in an oven at 80 °C for at least 12 h. Heat treatment of the resultant mixture was done in a tubular furnace at a temperature of 600 °C in the presence of N_2 gas atmosphere for 3 h. The materials were then centrifuged in diluted HCl for a period of one hour, filtered, and washed with water until a pH value of 7 was reached. Finally, the material was dried in the hot air oven at 100 °C overnight. Fig. 1a shows the schematic of KOH activation of HNT.

2.3 TEPA Impregnation on KOH-HNTs

Around 750 µL of TEPA solution is added to 20 ml of ethanol under stirring, and 1 g of alkali-activated HNTs (KOH-HNTs) is added to the ethanol/TEPA solution and stirred for 24 h at room temperature. Finally, the mixture was dried in an oven at 50 °C overnight. Fig. 1b shows the schematic for TEPA impregnation on HNTs.

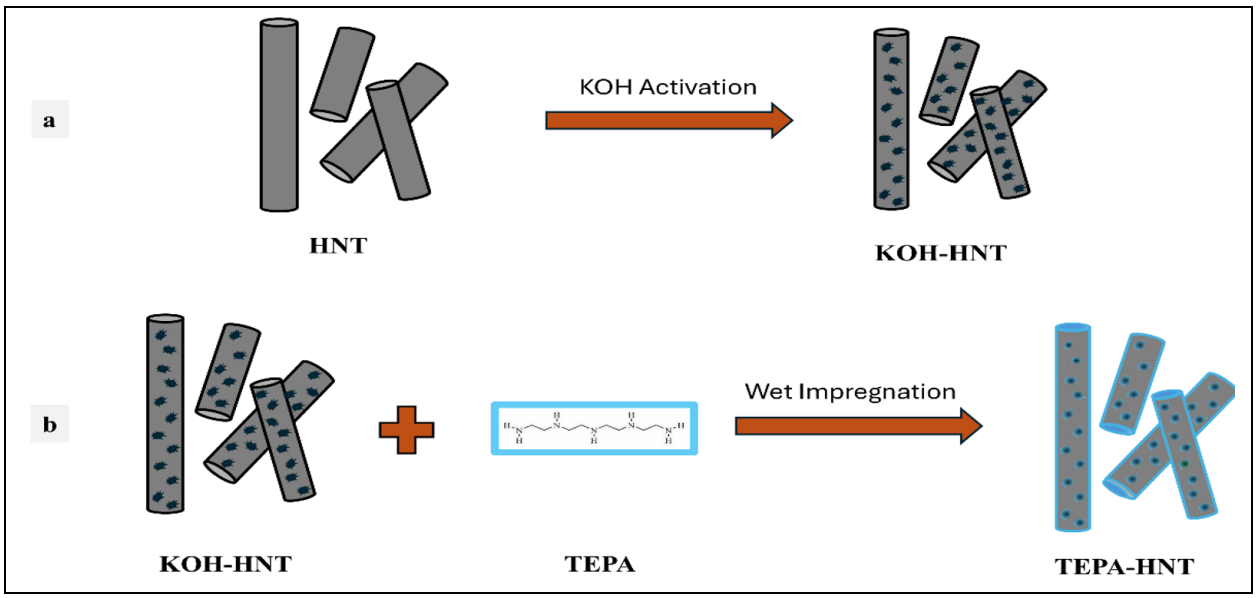


Fig. 1: Schematic diagram of HNT modification: (a) KOH activation and (b) TEPA modification

2.4 Characterization of Adsorbents

The morphology of HNT was characterized using scanning electron microscopy (Hitachi S 4800 FESEM) at 5 kV after coating the HNT with 0.5 nm gold by a Cressington sputter coater (208HR) at 20 mA for 1 min. The nanotubular lumen structure of HNT was characterized by transmission electron microscopy (TEM, Zeiss EM 912) at 120 kV. The modification of HNTs to KOH-HNTs and TEPA-HNTs was characterized by Fourier transform infrared spectroscopy (FTIR, Spectrum Two - Perkin Elmer) in the interval of 400–4000 cm^{-1} with a resolution of 1 cm^{-1}, as well as by scanning electron microscopy and energy dispersive X-ray analysis (SEM-EDAX, ZEISS Sigma-360) operated at 20 kV.

2.5 CO_2 Adsorption Studies

Synthesized flue gas with 15 vol.% CO_2 and remaining N_2 was used for adsorption studies (Muthumari *et al.* 2020). The carbon dioxide adsorption experiments were carried out at ambient temperature and at 0.5 psi gauge pressure. A certain amount of adsorbent (HNT, KOH-HNT, and TEPA-HNT) was taken into the sample chamber. The chamber is purged continuously with synthesized flue gas for 5 mins with 0.5 psi as inlet pressure and sealed for 1 h to ensure adsorption saturation. The samples were then analyzed for the amount of CO_2 adsorbed using the Indian Standard (IS-3025 part 61) method. In short, the adsorbed CO_2 was liberated by acidifying and heating the sample in a closed system. The liberated CO_2 was absorbed in an alkaline barium chloride solution, and the barium carbonate formed was determined by titration. For each of the three adsorbents, the adsorption experiments were conducted thrice and statistically compared for the amount of CO_2 absorbed per mg of adsorbent by one-way ANOVA.

3. RESULTS AND DISCUSSION

The electron microscopy images (Fig. 2) confirm the nanotubular nature of the HNT clay being used. The inner lumen diameter varies from 15–30 nm, the outer diameter from 50–100 nm, and the tube length from 100 nm to a few micrometers. The FTIR results of HNT (Fig. 3) show absorbance bands at 3696 cm^{-1} corresponding to stretching vibrations of inner surface O–H groups and those at 3621 cm^{-1} corresponding to inner O–H groups. Adsorbed water molecules on the surface are shown by a band at 3442 cm^{-1}. The band at 1660 cm^{-1} is due to H-O-H bending vibrations of water molecules in the interlayer space and of physically sorbed water. The band at 908 cm^{-1} corresponds to the water liberation mode. The band at 1008 cm^{-1} corresponds to Si-O stretching vibrations in distorted tetrahedral fragments. The bands at 760 cm^{-1} and 670 cm^{-1} correspond to Al–OH stretching vibrations. These bands have been previously reported for HNTs from various sources, confirming the characteristic features of HNT (Ramadass *et al.* 2018; Atyaksheva *et al.* 2021). The SEM-EDAX quantification results of HNTs (Figures 4a, 4d, and 4g) have indicated carbon impurities, which are further indicated by bands at 2900 cm^{-1} in FTIR results (Ramadass *et al*. 2018).

The FTIR results of KOH-HNT (Fig. 3) show that the bands in the range of 3621–3696 cm^{-1} are merged and less distinctive compared with HNT. Similarly, the bands in the range of 908–1008 cm^{-1} are also merged and less distinctive than those of HNT. This behavior may be attributed to the mechanism by which KOH activates HNT through reactions with oxygen-containing groups (Chen *et al*. 2020). In addition, alkali activation leads to dissolution of alumino-silicates into aluminate and

silicate oligomers to increase the porosity (Ahmed *et al.* 2020). The carbon impurities indicated by the band at 2900 cm^{-1} for HNT have disappeared in KOH-HNT due to alkali activation. The SEM-EDAX quantification results of KOH-HNT (Figures 4b, 4e, and 4h) have confirmed the disappearance of carbon impurities and the presence of potassium due to KOH modification. The SEM images of KOH-HNT (Figures 4b and 4e) in comparison to HNT (Figures 4a and 4d) indicate that KOH-HNT is more aggregated than HNT. This might be due to the dissolution of alumino-silicates due to KOH activation (Ahmed *et al.* 2020).

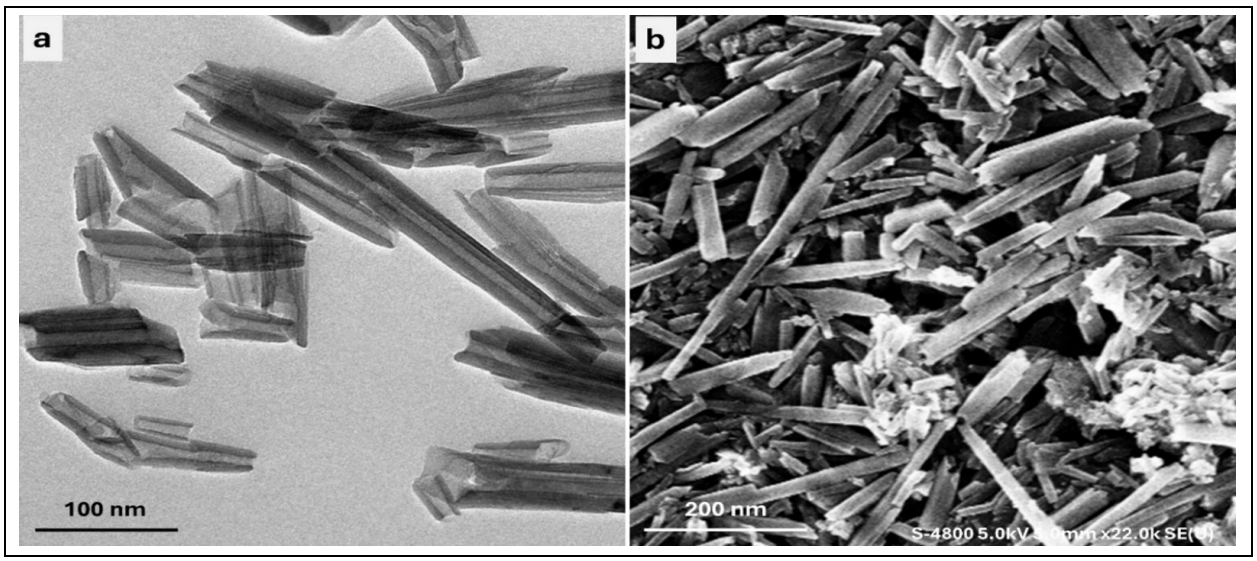


Fig. 2: (a) TEM and (b) SEM images of halloysite

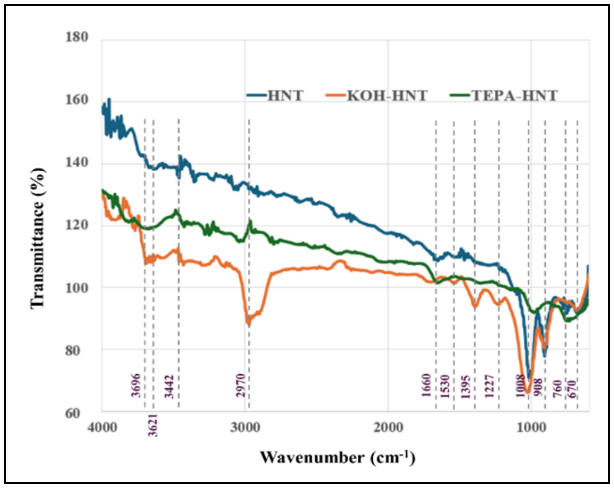


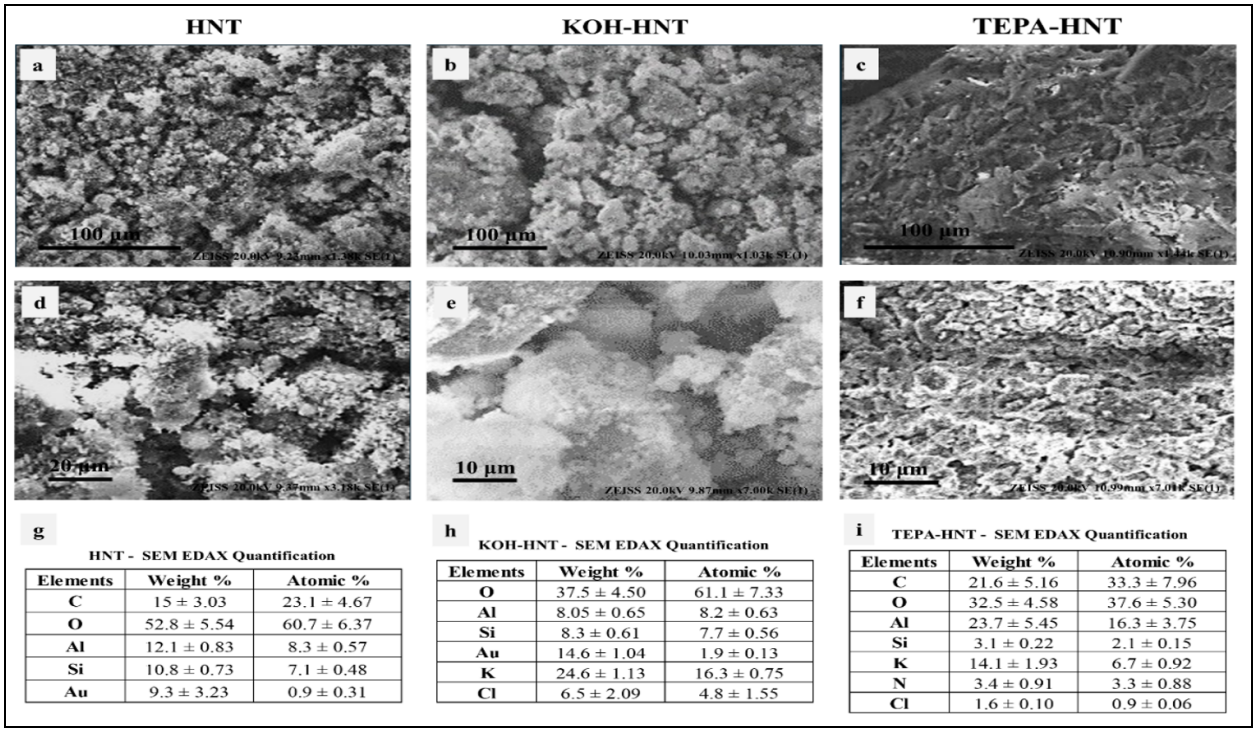
Fig. 3: FTIR spectra of HNT, KOH-HNT, and TEPA-HNT

The FTIR results of TEPA-HNT (Fig. 3) show unique bands from 2900 cm^{-1} to 2970 cm^{-1}, 1530 cm^{-1}, 1395 cm^{-1}, and 1227 cm^{-1}. The bands from 2900 cm^{-1} to 2970 cm^{-1} correspond to C–H asymmetric and symmetric vibration peaks (Liu *et al.* 2014). The -NH_2 and -NH bending vibration of TEPA are seen in the bands at 1530 cm^{-1} and 1395 cm^{-1}, respectively (Irani *et al.* 2017; Liu *et al.* 2014). The band at 1227 cm^{-1} can be attributed to the vibration of C–N (Liu *et al.* 2014). The SEM–EDAX quantification results of TEPA-HNT (Figures 4c, 4f, and 4i) have indicated the presence of carbon, nitrogen, and potassium. The FTIR results, along with SEM–EDAX quantification results, confirm KOH activation and the impregnation of TEPA on HNT.

The amount of CO_2 adsorbed by the adsorbents at 0.5 psi and ambient temperature is shown in Fig. 5. HNT has an adsorption capacity of 6.36 mmol CO_2/g, and the adsorption capacity of KOH-HNT increased to 7.50 mmol CO_2/g. TEPA-HNT showed the maximum adsorption capacity of 10.23 mmol CO_2/g of adsorbent, which is statistically significant in comparison with HNT and KOH-HNT. The observed higher CO_2 adsorption capacity by TEPA-modified HNT might be due to the synergistic effect of positively charged amine functional groups and the affinity of moisture towards TEPA. The positively charged amine functional groups help in the deagglomeration of HNT, which exposes more mesopores and thereby facilitates more CO_2 diffusion into the inner active sites (Guo *et al.* 2017). TEPA reacting with moisture and CO_2 results in the formation of bicarbonate and carbamate, thereby enhancing higher CO_2 adsorption capacity (Wang *et al.* 2020). Several authors have reported CO_2 adsorption capacity of HNT and modified HNT (Jana *et al.* 2015; Kim *et al.* 2016; Cai *et al.* 2015; Ramadass *et al.* 2018), which is lower when compared to TEPA-HNT. The difference might be due to the nature of HNT used, the type of amine used for HNT modification, and the change in CO_2 composition in the flue gas used for adsorption studies. Comparison of the above parameters with the current study is presented in

Table 1. It is clear from the table that halloysites from different geographical location deposits have different adsorption capabilities. Compared with APTES and PEI modifications, KOH modification and TEPA impregnation gave higher adsorption capabilities to HNT. It is important to note that one study (Ramadass *et. al*. 2018) showed closer adsorption capabilities to current results, which was done at high pressure of 30 bar, whereas the current study was done at near atmospheric pressure of 15.2 psi. Hence, KOH activation followed by TEPA impregnation for HNT is a facile method for enhancing the CO_2 capture capacity of halloysite.

In general, the post-combustion CO_2 capture commonly encounters high temperatures. Hence, the actual adsorption capacity of TEPA-HNT at those temperatures might be less than the reported value due to the exothermic nature of CO_2 adsorption (Singh *et al.* 2017). Moreover, TEPA-impregnated silica has shown higher thermal stability and can withstand up to 10 adsorption-desorption cycles (Kulkarni *et al.* 2023). As halloysite clay is made of alumino-silicates, similar stability is expected. Hence, TEPA-impregnated HNT can be explored further for high-temperature adsorption and its stability during various regeneration cycles.



Elements	Weight %	Atomic %
C	15 ± 3.03	23.1 ± 4.67
O	52.8 ± 5.54	60.7 ± 6.37
Al	12.1 ± 0.83	8.3 ± 0.57
Si	10.8 ± 0.73	7.1 ± 0.48
Au	9.3 ± 3.23	0.9 ± 0.31

Elements	Weight %	Atomic %
O	37.5 ± 4.50	61.1 ± 7.33
Al	8.05 ± 0.65	8.2 ± 0.63
Si	8.3 ± 0.61	7.7 ± 0.56
Au	14.6 ± 1.04	1.9 ± 0.13
K	24.6 ± 1.13	16.3 ± 0.75
Cl	6.5 ± 2.09	4.8 ± 1.55

Elements	Weight %	Atomic %
C	21.6 ± 5.16	33.3 ± 7.96
O	32.5 ± 4.58	37.6 ± 5.30
Al	23.7 ± 5.45	16.3 ± 3.75
Si	3.1 ± 0.22	2.1 ± 0.15
K	14.1 ± 1.93	6.7 ± 0.92
N	3.4 ± 0.91	3.3 ± 0.88
Cl	1.6 ± 0.10	0.9 ± 0.06

Fig 4: (a-f) SEM images and (g-i) SEM–EDAX quantifications of HNT, KOH-HNT, and TEPA-HNT, respectively

Table 1. Comparison of reported values of CO_2 absorbed by halloysite

Source of HNT	Chemical used for HNT modification	CO_2 percentage in the gas	Temperature of adsorption (°C)	CO_2 adsorbed (mmol/g)	Reference
Not mentioned	APTES	390 ppm (Ambient Air)	25	0.11	Cai *et al.* 2015
Natural Nano, Rochester, NY, USA	APTES	100%	50	0.09	Kim *et al.* 2016
Natural Nano, Rochester, NY, USA	PEI	100%	75	1.40	Kim *et al.* 2016
Jiangsu, China	PEI	390 ppm (ambient air)	25	1.25	Cai *et al.* 2015
Poochera, South Australia	None	Not mentioned	0	6.17	Ramadass *et al.* 2018
Applied Minerals, NY, USA	KOH	15%	25	7.50	Present work
Applied Minerals, NY, USA	TEPA	15%	25	10.23	Present work

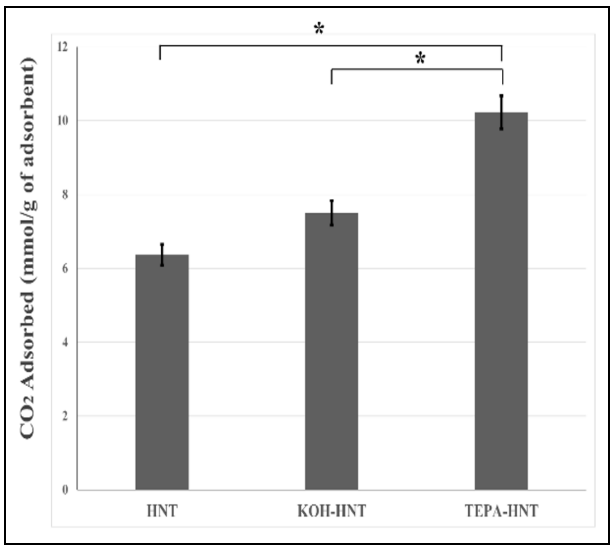


Fig. 5: CO_2 adsorbed by HNT, KOH-HNT, and TEPA-HNT (* indicates a significant difference with $p < 0.001$ based on one-way ANOVA; N = 3)

4. CONCLUSION

Halloysite was impregnated with TEPA after alkali activation using KOH to improve its CO_2 adsorption capacity. The adsorption capacity of halloysite significantly increased from 6.36 mmol CO_2/g of adsorbent to 10.23 mmol CO_2/g upon modification with TEPA. The high adsorption capacity of the modified HNT reported in the work, coupled with its low cost, makes TEPA-impregnated halloysite a promising nanomaterial for CO_2 capture. Further techno-economic studies on this adsorbent may yield a viable and flexible CO_2 capture system suitable for various process industries.

FUNDING

This research received no specific grant from any funding agency in the public, commercial, or not-for-profit sectors.

CONFLICTS OF INTEREST

The authors declare that there is no conflict of interest.

COPYRIGHT

This article is an open-access article distributed under the terms and conditions of the Creative Commons Attribution (CC BY) license (http://creativecommons.org/licenses/by/4.0/).

REFERENCES

Abdullayev, E. and Lvov, Y., Halloysite for controllable loading and release, *Dev. Clay Sci.,* 7, 554–605 (2016). https://doi.org/10.1016/B978-0-08-100293-3.00022-4

Ahmed, Z. K., Özlem, C., Yiannis, P., Andrew, H., Pascaline, P., Susan, A. B. and Alastair, T. M. M., Advances in alkali-activation of clay minerals, *Cem. Concr. Res*., 132, 106050 (2020). https://doi.org/10.1016/j.cemconres.2020.106050

Atyaksheva, L. F. and Kasyanov, I. A., Halloysite, natural aluminosilicate nanotubes: Structural features and adsorption properties (a review), *Pet. Chem*., 61(8), 932–950 (2021). https://doi.org/10.1134/S0965544121080119

Bertolino, V., Cavallaro, G., Milioto, S. and Lazzara, G., Polysaccharides/halloysite nanotubes for smart bionanocomposite materials, *Carbohydr. Polym*., 245, 116502 (2020). https://doi.org/10.1016/j.carbpol.2020.116502

Cai, H. H., Bao, F., Gao, J., Chen, T., Wang, S. and Ma, R., Preparation and characterization of novel carbon dioxide adsorbents based on polyethyleneimine-modified halloysite nanotubes, *Environ. Technol*., 36(10), 1273–1280 (2015). https://doi.org/10.1080/09593330.2014.984772

Chen, C., Zhang, S., Row, K. H. and Ahn, W. S., Amine–silica composites for CO_2 capture: A short review, *J. Energy Chem.*, 26, 868–880 (2017). https://doi.org/10.1016/j.jechem.2017.07.001

Chen, C. and Bhattacharjee, S., Trimodal nanoporous silica as a support for amine-based CO_2 adsorbents: Improvement in adsorption capacity and kinetics, Appl. Surf. Sci., 396, 1515–1519 (2017). https://doi.org/10.1016/j.apsusc.2016.11.200

Chen, W., Gong, M., Li, K., Xia, M., Chen, Z., Xiao, H., Fang, Y., Chen, Y., Yang, H. and Chen, H., Insight into KOH activation mechanism during biomass pyrolysis, *Appl. Energy*, 278, 115730 (2020). https://doi.org/10.1016/j.apenergy.2020.115730

Dhoke, C., Zaabout, A., Cloete, S. and Amini, S., Reactor configurations for adsorption-based CO_2 capture: A review, *Ind. Eng. Chem. Res*., 60, 3779–3798 (2021). https://doi.org/10.1021/acs.iecr.0c04547

Gargiulo, V., Alfe, M., Raganati, F., Lisi, L., Chirone, R. and Ammendola, P., BTC-based metal–organic frameworks for CO_2 adsorption, *Fuel*, 222, 319–326 (2018). https://doi.org/10.1016/j.fuel.2018.02.093

Guo, X. Z., Ding, L., Kanamori, K., Nakanishi, K. and Yang, H., Functionalization of hierarchically porous silica monoliths with polyethyleneimine (PEI) for CO_2 adsorption, *Microporous Mesoporous Mater*., 245, 51–57 (2017). https://doi.org/10.1016/j.micromeso.2017.02.076.

Irani, M., Jacobson, A. T., Gasem, K. A. M. and Fan, M., Modified carbon nanotubes/tetraethylenepentamine for CO_2 capture, *Fuel,* 206, 10–18 (2017). https://doi.org/10.1016/j.fuel.2017.05.087

Jacobson, M. Z., Review of solutions to global warming, air pollution and energy security, *Energy Environ. Sci.,* 2, 148–173 (2009). https://doi.org/10.1039/B809990C

Jana, S., Das, S., Ghosh, C., Maity, A. and Pradhan, M., Halloysite nanotubes capturing isotope selective atmospheric CO_2, *Sci. Rep*., 5, 8711 (2015). https://doi.org/10.1038/srep08711

Kim, J., Rubino, I., Lee, J. Y. and Choi, H. J., Application of halloysite nanotubes for carbon dioxide capture, *Mater. Res. Exp.,* 3, 045019 (2016). https://doi.org/10.1088/2053-1591/3/4/045019

Kulkarni, V., Panda, D. and Singh, S. K., Direct Air Capture of CO_2 over Amine-Modified Hierarchical Silica, *Ind. Eng. Chem. Res.,* 62(8), 3800-3811 (2023). https://doi.org/10.1021/acs.iecr.2c02268

Lee, S. Y. and Park, S. J., Solid adsorbents for carbon dioxide capture: A review, *J. Ind. Eng. Chem.,* 23, 1–11 (2015). https://doi.org/10.1016/j.jiec.2014.09.001

Leung, D. Y. C., Caramanna, G. and Maroto-Valer, M. M., Current status of carbon dioxide capture and storage technologies, *Renew. Sustain. Energy Rev.,* 39, 426–443 (2014). https://doi.org/10.1016/j.rser.2014.07.093

Liu, Q., Shi, Y., Zheng, S., Ning, L., Ye, Q., Tao, M. and Hu, Y., Amine-functionalized multi-walled carbon nanotubes for CO_2 capture, J. Energy Chem., 23, 111–118 (2014). https://doi.org/10.1016/S2095-4956(14)60124-8

Liu, Q., Shi, Y., Zheng, S., Tao, M., Hu, Y. and Shi, Y., Kinetic studies of CO_2 adsorption/desorption on amine-functionalized MWCNTs, Ind. Eng. Chem. Res., 53, 11677–11683 (2014a). https://doi.org/10.1021/ie502009n

Lou, F., Zhang, A., Zhang, G., Ren, L., Guo, X. and Song, C., Enhanced CO_2 sorption kinetics in amine-functionalized mesoporous silica, *Appl. Energy*, 264, 114637 (2020). https://doi.org/10.1016/j.apenergy.2020.114637

Mondal, M. K., Balsora, H. K. and Varshney, P., Progress and trends in CO_2 capture/separation technologies, *Energy*, 46, 431–441 (2012). https://doi.org/10.1016/j.energy.2012.08.006

Muthumari, P., Dhanalakshmi, J. and Ambedkar, B., CO_2 absorption in aqueous amine blends, *Chemosphere*, 276, 130519 (2021). https://doi.org/10.1016/j.chemosphere.2021.130159

Nie, L., Mu, Y., Jin, J., Chen, J. and Mi, J., Solid adsorbents for CO_2 capture from flue gas, *Chin. J. Chem. Eng.*, 26, 2303–2317 (2018). https://doi.org/10.1016/j.cjche.2018.07.012

Olajire, A. A., Functionalized porous adsorbents for CO_2 capture, *GHG Sci. Technol*., 7, 399–459 (2007). https://doi.org/10.1002/ghg.1657

Park, S., Ryu, J., Cho, H. Y. and Sohn, D., Halloysite nanotubes loaded with HKUST-1 for CO_2 adsorption, *Colloids Surf. A,* 651, 129750 (2022). https://doi.org/10.1016/j.colsurfa.2022.129750

Raganati, F., Miccio, F. and Ammendola, P., Adsorption of carbon dioxide for post-combustion capture, *Energy Fuels*, 35, 12845–12868 (2021). https://doi.org/10.1021/acs.energyfuels.1c01618

Ramadass, K., Singh, G., Lakhi, K. S., Benzigar, M. R., Yang, J. H., Kim, S., Almajid, A. M., Belperio, T. and Vinu, A., Halloysite nanotubes for high-pressure CO_2 capture, *Microporous Mesoporous Mater*., 277, 229–236 (2018). https://doi.org/10.1016/j.micromeso.2018.10.035

Saenz Cavazos, P. A., Hunter-Sellars, E., Lacomi, P., McIntyre, S. R., Danaci, D. and Williams, D. R., Evaluating solid sorbents for CO_2 capture, *Front. Energy Res.,* 11, 1167043 (2023). https://doi.org/10.3389/fenrg.2023.1167043

Santos, A. C., Ferreira, C., Veiga, F., Ribeiro, A. J., Panchal, A., Lvov, Y. and Agarwal, A., Halloysite nanotubes for life sciences applications, *Adv. Colloid Interf. Sci.,* 257, 58–70 (2018). https://doi.org/10.1016/j.cis.2018.05.007

Singh, G., Lakhi, K. S., Kim, I. Y., Kim, S., Srivastava, P., Naidu, R. and Vinu, A., Activated mesoporous biocarbons for high-pressure CO_2 adsorption, *ACS Appl. Mater. Interf.,* 9(35), 29782–29793 (2017). https://doi.org/10.1021/acsami.7b08797

Tharmavaram, M., Pandey, G. and Rawtani, D., Surface-modified halloysite nanotubes for multifunctional applications, *Adv. Colloid Interface Sci.,* 261, 82–101 (2018). https://doi.org/10.1016/j.cis.2018.09.001

Veerabadran, N. G., Price, R. R. and Lvov, Y. M., Clay nanotubes for encapsulation and sustained drug release, *NANO*, 2(2), 115–120 (2007). https://doi.org/10.1142/S1793292007000441

Veerabadran, N. G., Mongayt, D., Torchilin, V., Price, R. R. and Lvov, Y. M., Organized shells on clay nanotubes for controlled release, *Macromol. Rapid Commun.,* 30(2), 99–103 (2009). https://doi.org/10.1002/marc.200800510

Wang, Y., Guo, T., Hu, X., Hao, J. and Guo, Q., Mechanism and kinetics of CO_2 adsorption for TEPA-impregnated hierarchical mesoporous carbon in the presence of water vapor, *Powder Technol*., 368, 227-236 (2020). https://doi.org/10.1016/j.powtec.2020.04.062

Webley, P. A., Adsorption technology for CO_2 separation and capture, *Adsorp.*, 20, 225–231 (2014). https://doi.org/10.1007/s10450-014-9603-2

Wu, Y., Zhang, Y., Ju, J., Yan, H., Huang, X. and Tan, Y., Halloysite nanotubes–polysaccharide nanocomposites, *Polym.,* 11, 987 (2019). https://doi.org/10.3390/polym11060987

Ye, Q., Jiang, J., Wang, C., Liu, Y., Pan, H. and Shi, Y., Adsorption of low-concentration CO_2 on amine-modified CNTs, *Energy Fuels*, 26, 2497–2504 (2012). https://doi.org/10.1021/ef201699w

Zhang, H., Lai, X. and Wu, H., CO_2 adsorption of silane-modified halloysite, *Adv. Mater. Res.,* 989–994, 441–445 (2014). https://doi.org/10.4028/www.scientific.net/AMR.989-994.441

Zhao, P., Zhang, G., Yan, H. and Zhao, Y., Amine-functionalized solid adsorbents for post-combustion CO_2 capture, *Chin. J. Chem. Eng.,* 35, 17–43 (2021). https://doi.org/10.1016/j.cjche.2020.11.028